Magnetic tetrahedral intrasublattice interactions in the spinel family $Fe_xCu_{1-x}Rh_2S_4$

C. Boumford and A. H. Morrish
Department of Physics, University of Manitoba, Winnipeg, Canada R3T 2N2
(Received 30 August 1977)

Several compounds of the spinel $Fe_xCu_{1-x}Rh_2S_4$ with $x \leq 0.94$ have been prepared in order to study the magnetic interactions within the tetrahedral sites. The samples were investigated by x-ray, magnetization, and Mössbauer measurements at temperatures between 4.2 and 300 K. All the samples become antiferromagnets. No distortion of the spinel lattice was observed at any temperature. Ordering of the copper and iron ions for $0.46 \leq x \leq 0.7$ has been detected by an x-ray technique. Iron-rich compounds ($0.5 < x \leq 0.94$), cooled to 4.2 K in an external magnetic field of 18 kOe, exhibit remanences and displaced hysteresis loops reminiscent of spin glasses. Both susceptibility and isomer-shift measurements indicate a gradual change in valence state from ferric to ferrous iron as x is increased from 0.6 towards 1.0. Energy-band diagrams, consistent with the data, are proposed for the series.

I. INTRODUCTION

In the spinel structure, the cations occupy one tetrahedral (A) and two octahedral (B) sites per chemical formula unit. One approach to the study of the magnetic interactions on A sites is to arrange that all the B sites are occupied by diamagnetic ions. A good example of such a system is $Fe_xCu_{1-x}Rh_2S_4$. The trivalent rhodium ions occupy B sites only and, because the crystal field is large, are in the low-spin ground state (t_{2g}^6, e_g^0).

Previously, three compositions of the $Fe_xCu_{1-x}Rh_2S_4$ series have been investigated. One of the end members, $CuRh_2S_4$, is metallic and exhibits a temperature-independent paramagnetism.[1-3] The Van Vleck susceptibility of the Rh^{3+} ions is believed to be the main source of the paramagnetism.[4,5]

The middle member $Fe_{0.5}Cu_{0.5}Rh_2S_4$ is a p-type semiconductor and orders antiferromagnetically below about 140 K.[6] Low-temperature neutron-diffraction data shows that the copper and iron order onto the two interlocking face-centered-cubic A sublattices (A_1 and A_2), as indicated in Fig. 1. The copper ions on one A sublattice have zero magnetic moment. The iron ions on the other A sublattice are arranged into antiferromagnetic ordering of the second kind. It was concluded that the copper and iron ions were in the 1+ and 3+ valence states, respectively.

Several unsuccessful attempts have been made to prepare the other end member $FeRh_2S_4$.[7,8] Since both $CoRh_2S_4$ and $NiRh_2S_4$ are known to exist in spinel form,[7,9,10] this difficulty is surprising. Results on one sample prepared in our laboratory suggested that $FeRh_2S_4$ is an antiferromagnetic semiconductor with an ordering temperature of about 215 K.[11] The magnetic ordering appears to be similar to that for $CoRh_2S_4$, that is, an antiferromagnetic alignment of the A_1 and A_2 sublattice magnetizations. Unfortunately, the sample was not a single phase, and theoretical fits to the Mössbauer spectra were unsatisfactory. However, it was concluded that the iron was in the ferrous state, which suggested that the middle compound could have the formula $Fe_{0.5}^{2+}Cu_{0.5}^{2+}Rh_2^{3+}S_4^{2-}$.[8]

In Sec. II, the method used to prepare the several members of the $Fe_xCu_{1-x}Rh_2S_4$ family, and their characterization by x-ray techniques, will be described. Next, the magnetization measurements, including hysteresis loops, will be presented together with some in-

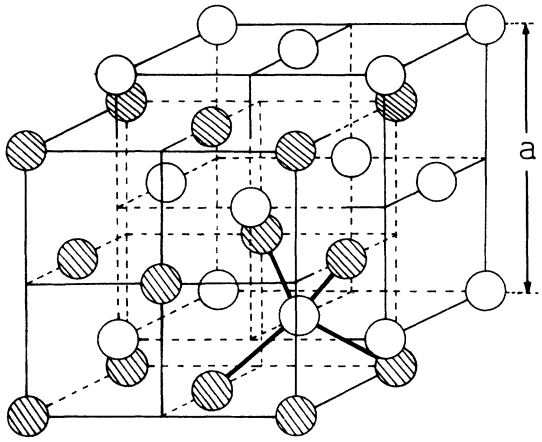

FIG. 1. Spinel A sites subdivided into two interpenetrating face-centered-cubic sublattices (one is represented by hatched circles the other by open circles).

terpretation of the results. Mössbauer-effect measurements and their implications will then be discussed, and finally, an energy-band diagram for the system will be proposed.

II. THE SAMPLES

Compounds with $x \leq 0.94$ were prepared by heating stiochiometric quantities of the elements in evacuated ampules. All the elements were 99.999% pure, and in addition the metals were reduced prior to weighing. Because sulfur has a high vapor pressure, the ampules were heated slowly to 400 °C and then held at this temperature for twelve hours before heating to 1050 °C. Initially sulfur vapor was clearly visible inside the tube, but disappeared after 3 days at 1050 °C. The samples were cooled to room temperature, hand ground for several minutes, sealed in evacuated ampules, and refired at 1050 °C. This treatment was repeated until x-ray analysis showed that a single-phase spinel structure had been achieved. Single-phase samples became increasingly more difficult to produce as the copper content was reduced, and it was not possible to prepare $FeRh_2S_4$ by this method. It has been proposed that the nobility of the rhodium may be the reason,[8] but since $CoRh_2S_4$, $NiRh_2S_4$, and $CuRh_2S_4$ can be prepared using similar techniques,[7] this suggestion seems unlikely.

Debye-Scherrer x-ray photographs of the samples with $0 \leq x \leq 0.94$ were indexed on a spinel unit cell. Accurate values of the lattice parameter a were found by plotting $a(\Theta)$ against the Nelson-Riley function and extrapolating to $\Theta = 90°$. The results are shown in Fig. 2, and establish that the variation of a with x is essentially linear.

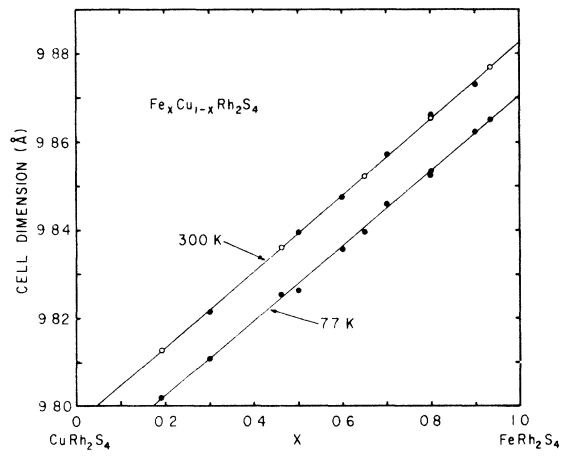

FIG. 2. Variation of the cell dimension with concentration. The closed circles represent the data points. The open circles correspond to samples enriched with ^{57}Fe; they were placed onto the room-temperature calibration curve.

The samples used as Mössbauer absorbers were prepared with iron enriched in the isotope ^{57}Fe. Since very small amounts of each compound were produced, the weighing errors became significant. Therefore, their composition was inferred from their lattice parameters as indicated by the open circles in Fig. 2.

A low-temperature powder diffractometer was used to measure the lattice parameters below room temperature. No evidence of any crystallographic distortion was found between 4.2 and 300 K. The results for $T = 77$ K are also plotted in Fig. 2.

By using iron-filtered cobalt radiation to depress the scattering factor of iron, the (420) superlattice reflection was detected for $0.45 \leq x \leq 0.7$. This observation provides direct evidence that the copper and iron ions are ordered on the two A sublattices for this compositional range.

III. MAGNETIZATION STUDIES

The magnetization of the compounds was determined with a vibrating sample magnetometer for temperatures from 4.2 to 300 K; the data indicated that all the samples ordered antiferromagnetically at some temperature within this range. Table I lists the molar Curie constant C_M and the paramagnetic Curie temperature Θ obtained from the measurements. If charge balance is preserved via the iron ions, then for $x > 0.5$ an ionic model predicts compounds with the form $(Fe^{2+}_{1-y}Fe^{3+}_{y})_x Cu^{1+}_{1-x} Rh^{3+}_2 S^{2-}_4$. The Curie constants predicted by theory are given in the last column of Table I; the agreement with the experimental values, corrected for the Van Vleck contribution by the Rh^{3+} ions, is satisfactory.

From the χ_m^{-1}-vs-T curves, the Néel temperatures of $Fe_{0.5}Cu_{0.5}Rh_2S_4$ and $Fe_{0.3}Cu_{0.7}Rh_2S_4$ were found to be 135 ± 5 and 130 ± 5 K, respectively. Above these temperatures both curves followed the Curie-Weiss law. The Néel temperatures for the compounds with $x > 0.5$ were not determined from similar plots since deviations from the Curie-Weiss law began at temperatures as high as 150 °C above distinct breaks in the curves. Similar results were found by Lotgering[12] for the $Co_xCu_{1-x}Rh_2S_4$ series. This behavior is evident in Fig. 3, which shows graphs of χ_M vs T.

The high Neel temperature of $Fe_{0.3}Cu_{0.7}Rh_2S_4$, a compound with a relatively low concentration of magnetic ions, suggests that an indirect exchange interaction via a polarized band is operating. A transition to metallic behavior as the iron content is reduced is to be expected since the end member $CuRh_2S_4$ is known to be a p-type conductor.[13] The possibility of a moment associated with the copper ions in the iron deficient compounds (that is, localized Cu^{2+} ions) is discounted because no evidence of long-range order in $CuRh_2S_4$ has been found, and further, its susceptibility appears to be just the sum of diamagnetic, Pauli paramagnetic, and Van Vleck contributions.

TABLE I. Experimenal molar Curie constants (emu deg/Oe), paramagnetic Curie temperatures (K), and the theoretical Curie constants (emu deg/Oe) for $Fe_xCu_{1-x}Rh_2S_4$.

	Observed		With Van Vleck correction		Calculated		
x	C_M	Θ	C_M	Θ	$C_M(Fe^{3+})$	$C_M(Fe^{2+})$	$C_M(Fe^{3+}:Fe^{2+})$
0.3	1.97	−410	1.57	−355	1.31	0.90	1.31
0.5	2.50	−412	2.09	−367	2.19	1.50	2.19
0.6	2.68	−310	2.34	−284	2.63	1.80	2.33
0.7	2.78	−278	2.46	−256	3.07	2.10	2.49
0.8	3.06	−355	2.69	−326	3.50	2.40	2.70
0.9	3.45	−427	3.02	−393	3.93	2.70	2.82
1.0					4.38	3.00	3.00

As the iron content increases above $x = 0.5$, iron ions replace copper ions on the A_2 sublattice and two strong competing antiferromagnetic interactions are expected to be present in the compounds. One is the A_1-A_1 long path (Fe-S-Rh-S-Rh-S-Fe) superexchange interaction, already proposed by Plumier and Lotgering[6] for $Fe_{0.5}Cu_{0.5}Rh_2S_4$. The second is the A_1-A_2 (Fe-S-Rh-S-Fe) superexchange interaction which dominates in the two cobalt rhodium spinels $CoRh_2O_4$ (Ref. 14) and $CoRh_2S_4$.[12]

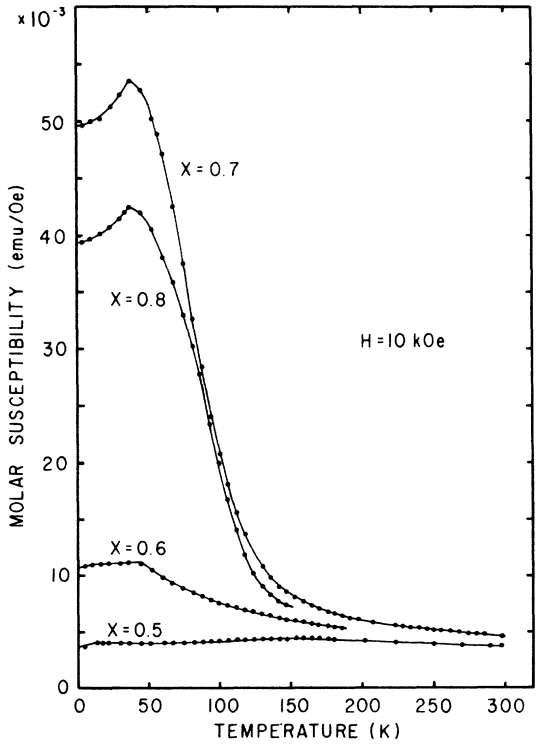

FIG. 3. Temperature dependence of the molar susceptibility at $H = 10$ kOe for the series $Fe_xCu_{1-x}Rh_2S_4$.

As discussed at the beginning of this section, the Curie constants (Table I) indicate that the valence state of the iron ions changes from ferric to ferrous as x increases. Mössbauer measurements, to be described in Sec. IV, confirm this valence change, and moreover show that the Néel temperature undergoes a sharp drop as soon as x exceeds 0.5. Therefore, the shift in the electron distribution which accompanies the valency change apparently leads to a significant weakening of the first (A_1-A_1) superexchange coupling.

In the two cobalt spinels,[12,14] the second (A_1-A_2) interaction leads to a simple antiparallel alignment of the A_1- and A_2-sublattice magnetizations. In the $Fe_xCu_{1-x}Rh_2S_4$ series, the A_1-A_2 interaction may be expected to become increasingly important as more iron ions occupy A_2 sites, and to become larger than the A_1-A_1 interaction at the higher iron concentrations.

The strong A_1-A_1 and A_1-A_2 competing interactions may be anticipated to lead to a number of new interesting effects, and indeed further magnetization experiments confirmed this expectation. Oddly enough, many of these features are somewhat similar to those observed for a spin glass. At $T = 4.2$ K, these include zero remanent moment for $x = 0.6$, a remanence and a displaced hysteresis loop when the sample is cooled in a magnetic field, an increase in the remanence, (although not linear) for $0.5 < x < 0.8$, and creep, that is, a change in the magnetization in an applied field with time. The magnetization at 4.2 K as a function of applied field for samples with and without an 18-kOe field applied during cooling to liquid-helium temperatures is shown for $x = 0.6$, 0.7, 0.8, and 0.9 in Fig. 4. For completeness, it should be mentioned that the magnetization versus field curves at 4.2 K for $x \leq 0.5$ exhibited no hysteresis, and were identical, with or without a magnetic field applied during cooling.

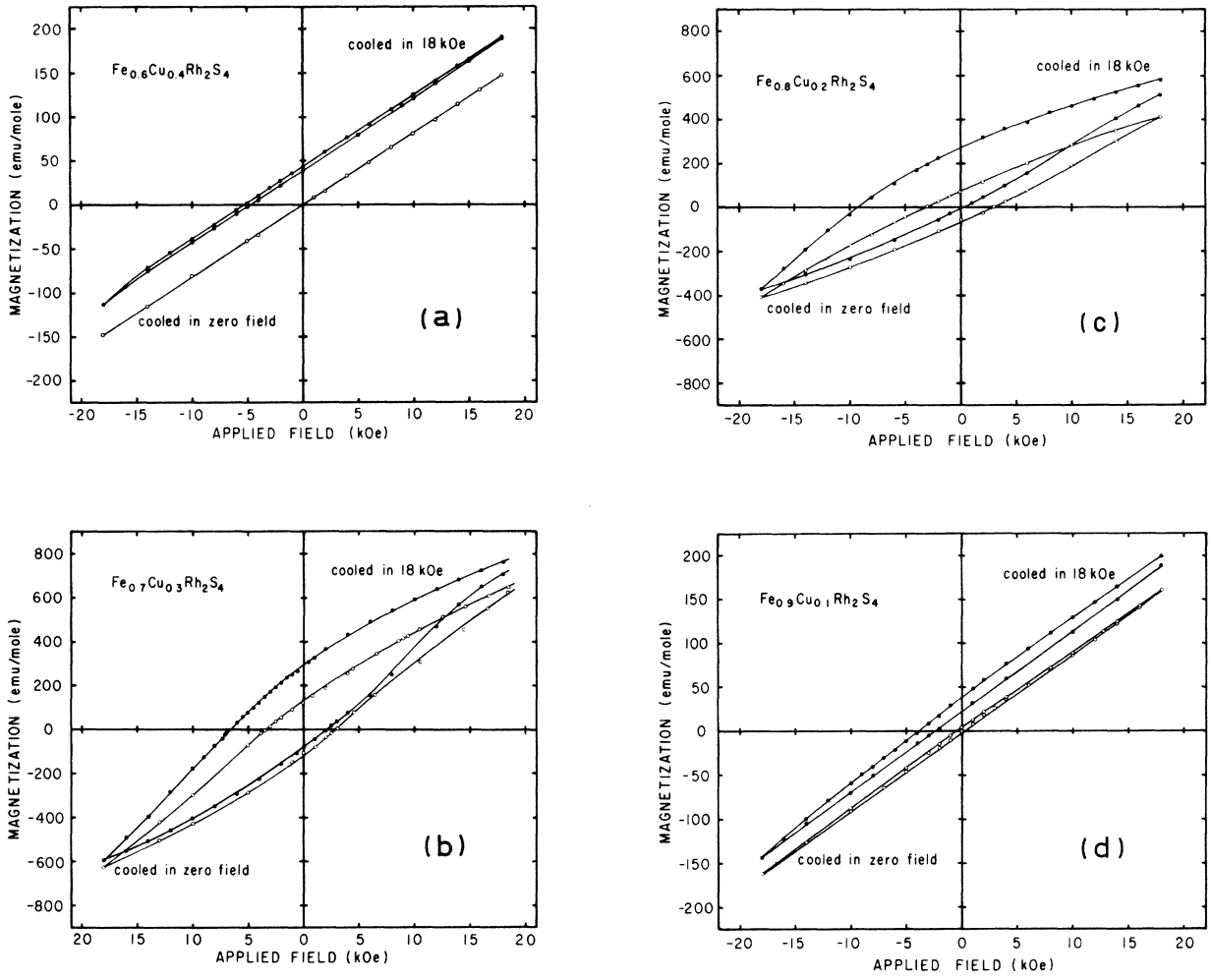

FIG. 4. Magnetization as a function of applied field at 4.2 K for four members of the series $Fe_xCu_{1-x}Rh_2S_4$.

The compound $Fe_{0.6}Cu_{0.4}Rh_2S_4$ will now be considered in some detail [Fig. 4(a)]. Since the x-ray measurements showed that the iron and copper ions are ordered to some degree on the A_1 and A_2 sublattices, it follows that most of the iron is arranged antiferromagnetically on the A_1 sublattice, and the excess replaces copper on the A_2 sublattice. The interaction between the excess iron ions and the antiferromagnetic A_1 sublattice then leads to a zero net moment. Whether the iron ions on the A_2 sites have a simple Néel configuration, or whether they are equally distributed over a number of equivalent directions cannot be determined from the experimental results. However, it is clear that most if not all of the excess iron ions are frozen into position at 4.2 K by an energy barrier sufficiently large to prevent realignment by an 18-kOe applied field.

The displaced hysteresis loop could be produced by one or other of the following two mechanisms. In the first, the iron ions on the A_2 sites are assumed to be strongly coupled to the A_1 sublattice, and to have a number of magnetically equivalent directions. Just below some ordering or blocking temperature T_B, this coupling will be small, and the application of an external magnetic field will lead to a net magnetic moment. On further cooling, the excess spins will relax from the field direction towards the nearest easy direction of magnetization. On removal of the external field at 4.2 K, a nonzero remanence will remain.

The second mechanism would apply if the lowest-energy state of the system required that each A_2-site spin has a unique orientation with respect to the A_1-sublattice antiferromagnetic axis. In the ordering scheme for the A_1 sublattice proposed by Plumier and Lotgering,[6] the ionic moments are collinear with one set of the ⟨100⟩ directions. On cooling with no external field applied, the ⟨100⟩ directions of the crystallites will be equally populated. However, on cooling

with an external field applied, the field induced alignment of the A_2 spins will lead, through exchange coupling, to the selection of a preferred antiferromagnetic axis for the A_1 sublattice. On removal of the external field at low temperatures, the A_2-site spins will be aligned with this A_1-sublattice axis, and a remanence will result. For either mechanism, the high-field cooled M-vs-H curves will consist of a hard ferromagnetic component superposed on the zero-field cooled antiferromagnetic component, and the displaced hysteresis loop shown in Fig. 4(a) will be the result.

When $x = 0.7$, the increase in the iron concentration on the A_2 sublattice may be expected to produce an increase in the remanence, as observed [Fig. 4(b)]. The increase in the hysteresis implies a weakening in the locking mechanism, and is presumably to be associated with the change in the electron distribution of the iron ions.

As x is increased above 0.7, the magnetic ordering is likely to become complex until the end member is approached. Then since the A_1-A_2 interaction will dominate, the magnetization of the A_1 sublattice will be antiparallel to that of the A_2 sublattice.[8] At some value of x the A_1-A_1 and A_1-A_2 interactions will be comparable, and a maximum in the susceptibility is expected below T_N. From Fig. 3, this point appears to be reached in the region $0.7 < x < 0.8$.

For $x > 0.7$, the energy barrier for spin reorientation on the A_2 sublattice would tend to increase. However, the copper ions effectively act to produce holes in the magnetic A_2 sublattice, and the energy barriers may be reduced for the near neighbors. These iron spins may then be locked into a preferential alignment on cooling with an external field present. Certainly, a reduction in the remanence and hysteresis is observed for $x > 0.7$, as shown in Figs. 4(c) and 4(d). A summary of the variation in some of the magnetic parameters for $0.5 \leq x \leq 0.9$ is presented in Fig. 5.

At a sufficiently high temperature T_B, thermal energy will be sufficient to overcome the energy barrier against spin reorientation, and the remanent moment will disappear. The remanent moment was observed to approach zero gradually as the temperature was increased above 4.2 K, and hence indicates a distribution in the heights of the energy barriers, which is to be expected since they will depend on the number, position, and orientation of near and distant magnetic neighbors. Within the experimental accuracy, T_B was found to be about 35 ± 5 K for all the iron-rich samples.

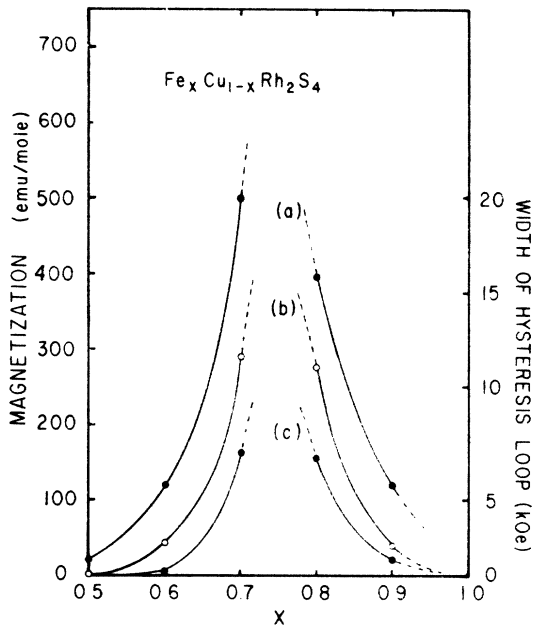

FIG. 5. Compositional dependence (a) of the magnetization measured with $H = 10$ kOe, (b) of the width of the hysteresis loop at zero magnetization, and (c) of the remanent magnetization, all at $T = 4.2$ K. For (a) and (b) the samples were cooled to 4.2 K without any external magnetic field applied, whereas for (c) the samples were cooled in an external field of 18 kOe.

IV. MÖSSBAUER STUDIES

Mössbauer spectra were recorded at temperatures from 2 to 300 K. As will become evident, the results were generally consistent with the magnetization investigation. However, the low temperature spectra of the iron-rich compounds consisted of broad overlapping lines, and the computer fitting was unreliable.

Examples of spectra for $Fe_{0.19}Cu_{0.81}Rh_2S_4$ are shown in Fig. 6. Above the ordering temperature the isomer shift (δ) and the lack of quadrupole splitting (ϵ) suggests that the iron ions are in the ferric state.[15] Below the ordering temperature the slightly broadened six-line spectrum indicates that the iron ions occupy a single lattice site, but are surrounded by a distribution of magnetic and diamagnetic neighbors. A spectrum in an external magnetic field of 50 kOe applied parallel to γ-ray direction is shown in Fig. 4(d). The presence of the 2 and 5 lines ($\Delta m = 0$ transitions) is expected for an antiferromagnetic powder. The angular distribution of the hyperfine fields with respect to the applied field produces the observed line broadening; since the splitting of the nuclear levels is proportional to $m_I H$, this broadening is most pronounced for the outer lines.[16] Similar results were found for the middle of the series ($x = 0.5$) except that spectra recorded without an applied field showed no line broadening at any temperature. Data from samples with $x \leq 0.5$ are summarized in Table II.

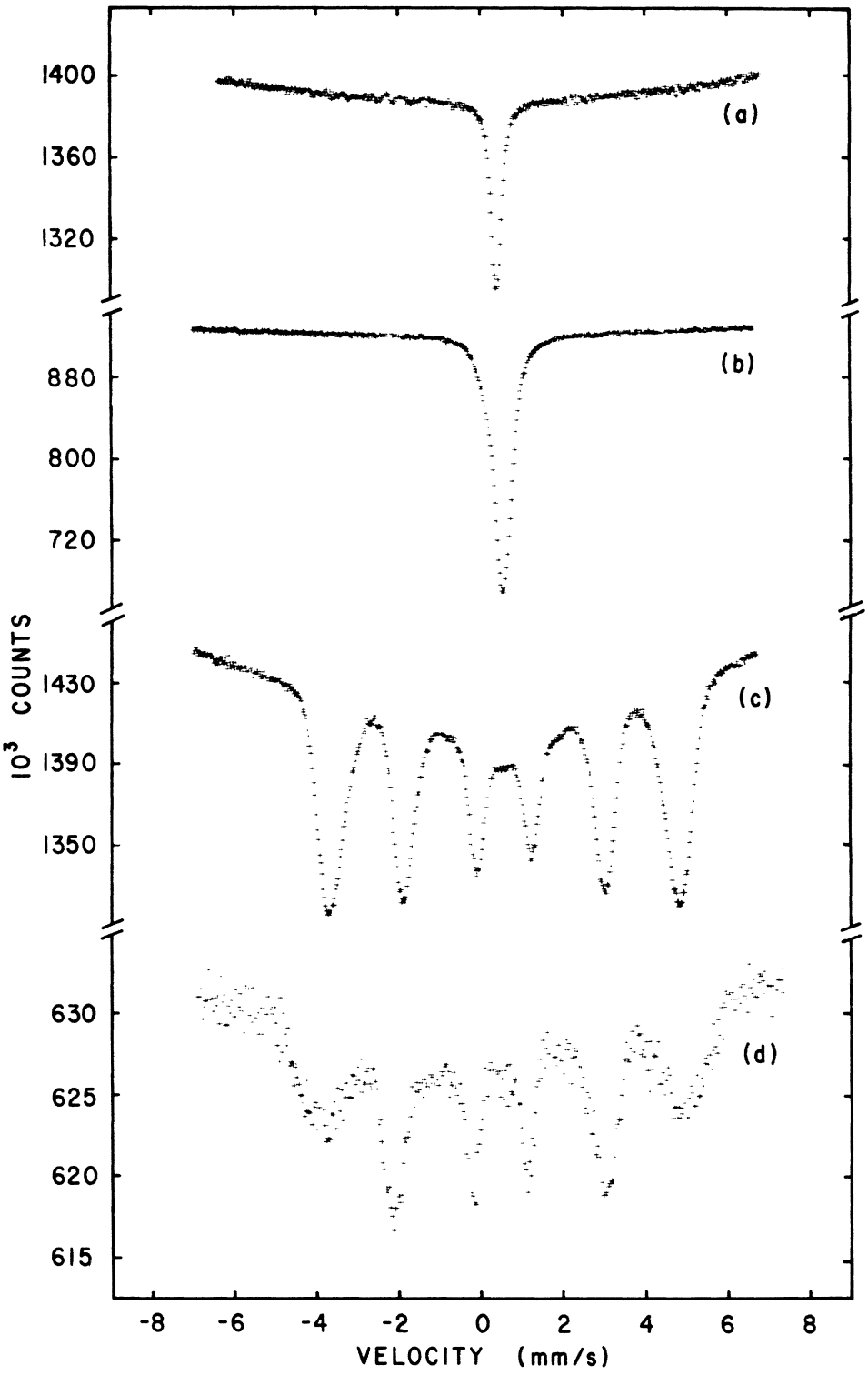

FIG. 6. Mössbauer spectra of $Fe_{0.19}Cu_{0.81}Rh_2S_4$ in zero-applied magnetic field at the temperatures of (a) 300, (b) 77, (c) 4.2 K, and (d) in a magnetic field of 50 kOe applied parallel to the propagation direction of the γ ray at $T = 4.2$ K.

TABLE II. Mössbauer parameters for $Fe_xCu_{1-x}Rh_2S_4$ at 4.2 K.

x	ϵ(mm/s)*	δ(mm/s)	H_{hf} (kOe)
0.19	0.00	0.60	264
0.30	0.00	0.60	290
0.45	0.00	0.59	292
0.50	0.00	0.59	296
0.60	0.00	0.60	290
0.65	0.40	0.61	285
0.70	0.00	0.60	275
	0.22	0.80	244

*Relative to Cr.

For a sample with $x > 0.5$, the magnetization experiments suggested that the compounds had the ionic form $(Fe^{2+}_{1-y}Fe^{3+}_{y})_xCu^{1+}_{1-x}Rh^{3+}_2S^{2-}_4$. The Mössbauer spectra from samples with $0.5 < x < 0.7$ consisted of one broadened six-line pattern below the ordering temperature and a broadened single line above. A distribution in magnetic neighbors would contribute to line broadening, as would any electron localization to form Fe^{3+} and Fe^{2+}. From Table II, it may be noted that the isomer shifts increase and the hyperfine fields decrease as x is increased in the compositional range. The data are consistent with fast-electron exchange between ferric and ferrous ions which leads to a single charge averaged pattern; a similar suggestion was made for iron on the A sites of $Fe_{1-x}Cu_xCr_2S_4$.[17]

When $x = 0.7$, two distinct overlapping patterns are observed in the spectrum at 4.2 K; the implication is that the electron hopping frequency has decreased. One pattern has a zero quadrupole shift and an isomer shift appropriate to that for ferric ions; the other has a significant quadrupole shift and a substantially larger isomer shift (Table II) which are consistent with those for ferrous ions. At $T = 77$ K, the paramagnetic absorption consists of a singlet and a quadrupole doublet; as the temperature is raised the doublet disappears. The ionic compound would have the formula $Fe^{2+}_{0.4}Fe^{3+}_{0.3}Cu^{1+}_{0.3}Rh_2S_4$, and the relative intensity of the two patterns is close to a 4-to-3 ratio at both 77 and 4.2 K.

As the iron content is increased further, the spectra become much more complex, as illustrated by the spectra for $Fe_{0.8}Cu_{0.2}Rh_2S_4$ shown in Fig. 7. Note the appearance of a quadrupole splitting at room temperature. Although apparently a simple doublet, the spectra develop structure as the temperature is lowered, and at 77 K at least two and possibly more overlapping doublets are present. Below T_N the spectra can be fitted with two very broad overlapping six-line patterns.

With further increase in iron content, the samples became increasingly more difficult to prepare as a single-phase spinel structure and the limiting compound achieved was $Fe_{0.94}Cu_{0.06}Rh_2S_4$. The apparently simple quadrupole-split doublet observed at $T = 300$ K for this compound became highly complex, with large broadened overlapping lines, as the temperature was lowered. These spectra were similar to those observed for $FeCr_2S_4$.[18] Later work on $FeCr_2S_4$ established that strains introduced by the thermosetting plastic in which the sample was sealed were a major source of the broad lines.[19] Since the $Fe_xCu_{1-x}Rh_2S_4$ absorbers used in the current experiment were in the form of loose powders, their spectra are not the result of a externally applied stress. Although no crystalline distortion was detected by x rays, it is conceivable that internal stresses at the iron sites lead to the observed Mössbauer spectra, and indeed may be a major factor in limiting the amount of iron that can be incorporated into the lattice.

In order to test the "excess spin" model proposed to account for the remanence and displaced hysteresis loop when a sample was cooled in an external field, the following experiment was performed. A sample of $Fe_{0.65}Cu_{0.35}Rh_2S_4$ was cooled from room temperature to 4.2 K in a 50-kOe external field and a Mössbauer spectrum was collected without removing the field. If the excess spins are aligned with the external field, then their hyperfine fields will be reduced by 50 kOe and their 2 and 5 lines will be absent for a longitudinal geometry. The spectrum obtained, and, for comparison, one in zero applied field, are shown in Fig. 8. A pattern with a smaller hyperfine field and relatively small 2,5 lines is indeed superposed on the broadened six-line pattern associated with the antiferromagnetic A_1 sublattice.

The isomer shift at room temperature is plotted as a function of the iron concentration in Fig. 9. Values characteristic for Fe^{3+} ions change to those typical for Fe^{2+} ions when x exceeds 0.5.

Figure 10 shows the variation of the ordering temperature T_N with iron content, as determined using the Mössbauer effect. As expected, the fully ordered compound $Fe_{0.5}Cu_{0.5}Rh_2S_4$ has the maximum Neel temperature. A further increase in T_N occurs as x approaches unity; the samples then presumably tend towards the $CoRh_2S_4$-type structure. The Neel temperatures for $x < 0.5$ are relatively high, and confirm the values obtained from the magnetization measurements.

V. PROPOSED ENERGY-BAND DIAGRAMS

Since the experimental data provides strong evidence that the iron in $Fe_{0.5}Cu_{0.5}Rh_2S_4$ is all in the ferric state, an energy-band scheme based on the ideas of Lotgering[4,9,12,13] rather than those of Goodenough[2] has been chosen. The energy-band diagrams proposed for the $Fe_xCu_{1-x}Rh_2S_4$ family are shown in Fig. 11.

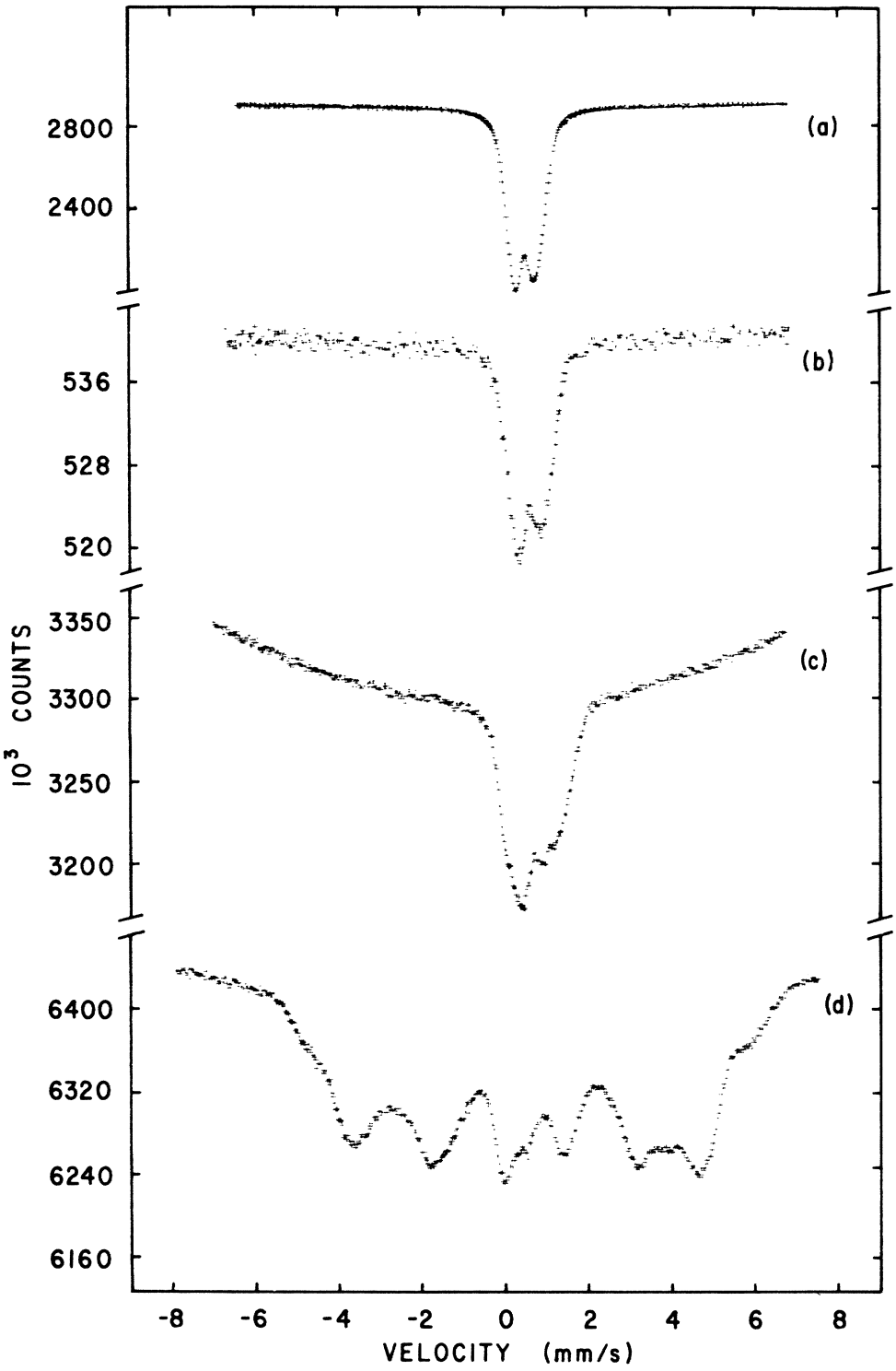

FIG. 7. Mössbauer spectra of $Fe_{0.8}Cu_{0.2}Rh_2S_4$ at (a) 300, (b) 200, (c) 77, and (d) 4.2 K.

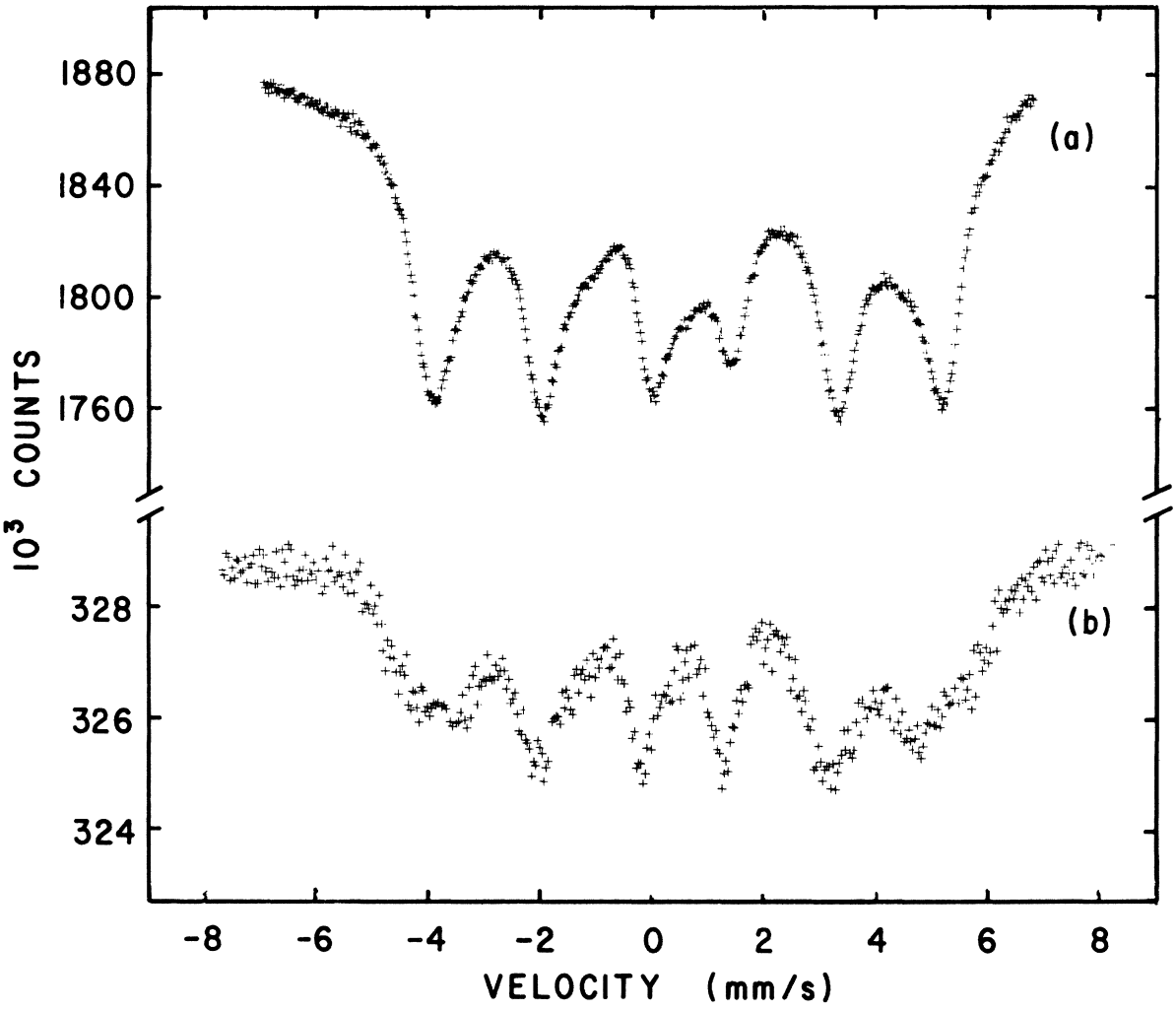

FIG. 8. Mössbauer spectra of $Fe_{0.65}Cu_{0.35}Rh_2S_4$ at 4.2 K (a) in zero external magnetic field and (b) in a longitudinal field of 50 kOe.

Here the energy E is plotted versus the density of states g so that $\int g\,dE$ gives the number of states per molecule.

The 4s electrons of the cations give rise to a conduction band and the 3p orbitals of the sulfur ions form a broad valence band.[20] The 3d electrons are more localized and hence lie in narrow energy bands. The Cu^{1+} ions have a filled 3d band that lies far below the top of the valence band. The Rh^{3+} band is also filled and overlaps the filled part of the valence band for all members of the series. The Fe^{2+} band lies in the gap between the bottom of the conduction band and the top of the valence band; an occupied state represents an Fe^{2+} ion, and an unoccupied state an Fe^{3+} ion. The position of the Fermi level E_F is also indicated.

The band scheme for $CuRh_2S_4$ was proposed by Lotgering.[12] The valence band has one hole per molecule, which gives a p-type conductivity and a small temperature-independent susceptibility. The hole is associated with sulfur 3p states corresponding to the formal valencies $Cu^{1+}Rh_2^{3+}S_3^{2-}S^{-}$.

As iron replaces copper, an empty Fe^{2+} band (Fe^{3+} ions) appears in the band gap, and the number of holes in the valence band decreases. The compounds for $0 \leq x \leq 0.5$ can be represented by the valence formula $Fe_x^{3+}Cu_{1-x}^{1+}Rh_2^{3+}S_{3+2x}^{2-}S_{1-2x}^{-}$. For $Fe_{0.5}^{3+}Cu_{0.5}^{1+}Rh_2^{3+}S_4^{2-}$ the valence band is completely filled, and it is a semiconductor rather than a metal. Plumier and Lotgering[6] made resistivity measurements on two samples with $x = 0.5$ and found one was a p-type and the other an n-type semiconductor. On the basis of the band model, a small deviation in composi-

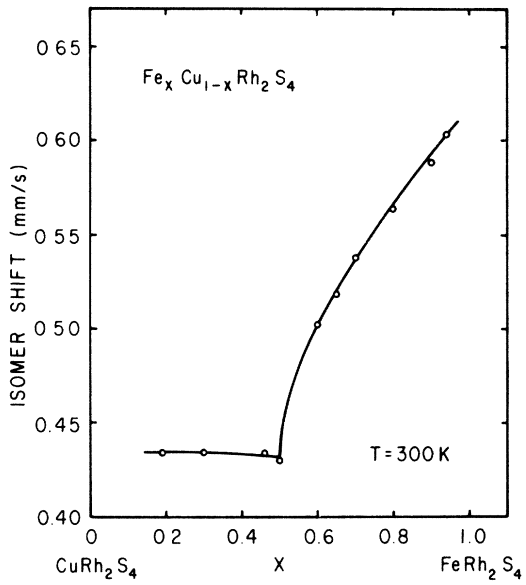

FIG. 9. Compositional dependence of the isomer shift of $Fe_xCu_{1-x}Rh_2S_4$. The full curve is drawn through the data points for clarity.

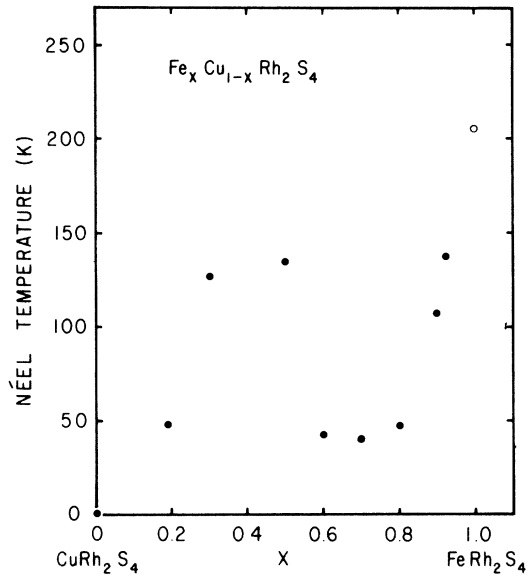

FIG. 10. Compositional dependence of the ordering temperature of $Fe_xCu_{1-x}Rh_2S_4$. The ordering temperature of $FeRh_2S_4$ was taken from Ref. 8.

tion from $x = 0.5$ would account for these observations.

For $0.5 < x < 1$ the Fe^{2+} band is partially filled producing a mixture of ferric and ferrous ions. At low temperatures, electron localization at the iron ions is detected for $x = 0.7$ in Mössbauer experiments. In this band model, $FeRh_2S_4$ is predicted to be a semiconductor. Indeed, resistivity measurements on a nonsingle phase sample do show a semiconducting behavior.[8] Further, magnetization measurements indicate that the ions are ferrous and possess a $CoRh_2S_4$-type of ordering.

VI. CONCLUSIONS

The compounds $Fe_xCu_{1-x}Rh_2S_4$ were shown to exist in spinel form for $0 \leq x \leq 0.94$ and no distortions from the spinel structure were found for any member of the series between 4.2 K and room temperature. By taking advantage of the depression of the scattering factor of iron close to its K-absorption edge, superlattice lines characteristic of spinel A site ordering were found in the concentration range $0.46 \leq x \leq 0.7$, in agreement with earlier neutron-diffraction work on $Fe_{0.5}Cu_{0.5}Rh_2S_4$.

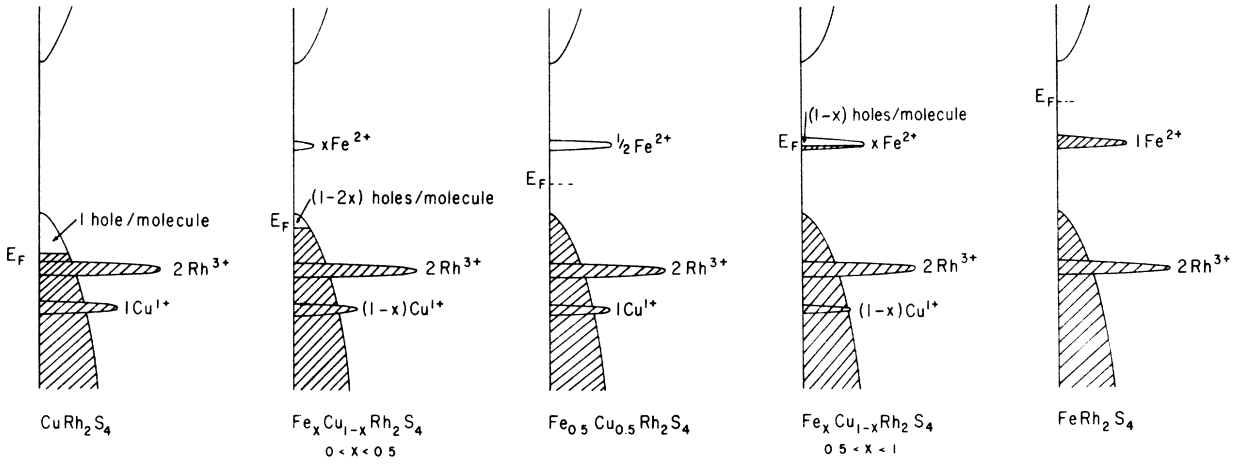

FIG. 11. Energy level schemes proposed for the $Fe_xCu_{1-x}Rh_2S_4$ series. The energy is plotted vs the density of states.

Magnetization measurements showed the series to be antiferromagnetic although a spontaneous moment could be induced for $0.5 < x \leq 0.94$ by cooling through the Néel point in an externally applied magnetic field. This moment was "locked in" at low temperatures producing hysteresis loops which were displaced along the field axis. An explanation of this frozen moment was given, based on a model with excess iron spins distributed on the copper A_2 sublattice.

Both susceptibility measurements above the ordering temperature and isomer-shift measurements at room temperature indicate a gradual change in valence state of the iron from Fe^{3+} for $x \leq 0.5$ to Fe^{2+} as $x \rightarrow 1$. Low-temperature Mössbauer measurements showed evidence for the presence of both Fe^{2+} and Fe^{3+} ions for $x \geq 0.7$, with intensity ratios in good agreement with those required for ionic charge balance. The low-temperature spectra became increasingly complex as $x \rightarrow 1$, the broad overlapping lines preventing theoretical fitting for $x \geq 0.9$; it was suggested that strain induced at the individual iron sites may be the origin of this complexity in the spectra.

Energy-band diagrams were proposed that were consistent with the compositional dependence of the conductivity, valence states, and magnetic data.

ACKNOWLEDGMENTS

We wish to thank Dr. I. Maartense and Dr. M. R. Spender for several helpful suggestions and discussions. This research was supported by the National Research Council of Canada.

[1]P. R. Locher and R. P. van Stapele, J. Phys. Chem. Solids 31, 2643 (1970).
[2]J. B. Goodenough, J. Phys. Chem. Solids 30, 261 (1969).
[3]G. Blasse, Phys. Lett. 19, 110 (1965).
[4]F. K. Lotgering and R. P. van Stapele, J. Appl. Phys. 39, 417 (1968).
[5]G. Blasse and D. J. Schipper, J. Inorg. Nucl. Chem. 26, 1467 (1964).
[6]R. Plumier and F. K. Lotgering, Solid State Commun. 8, 477 (1970).
[7]R. E. Tressler and V. S. Stubican, *Sulfospinels*, Nat. Bur. Stand. (U.S.) Spec. Publ. No. 364 (U. S. GPO, Washington, D. C., 1972), pp. 695–702.
[8]M. R. Spender, Ph.D. thesis (University of Manitoba, 1973) (unpublished).
[9]F. K. Lotgering, Philips Res. Rep. 11, 190 (1956).
[10]P. Gibart, J. L. Dormann, and Y. Pellerin, Phys. Status Solidi 36, 187 (1969).
[11]M. R. Spender and A. H. Morrish, *Proceedings of the Fifth International Conference on Mössbauer Spectroscopy* (Czechoslovakian Atomic Energy Commission, Prague, 1975), pp. 125–129.
[12]F. K. Lotgering, J. Phys. Chem. Solids 30, 1429 (1969).
[13]F. K. Lotgering, J. Phys. Chem. Solids 29, 699 (1968).
[14]G. Blasse, Philips Res. Rep. 18, 383 (1963).
[15]M. Eibschütz, S. Shtrikman, and V. Tenebaum, Phys. Lett. A 24, 563 (1967).
[16]H. N. Ok, W. R. Helms, and J. G. Mullen, Phys. Rev. 187, 704 (1969).
[17]G. Haacke and A. J. Nozik, Solid State Commun. 6, 363 (1968).
[18]M. R. Spender and A. H. Morrish, Can. J. Phys. 50, 1125 (1972).
[19]M. R. Spender and A. H. Morrish, Solid State Commun. 11, 1417 (1972).
[20]F. K. Lotgering, R. P. van Stapele, G. H. A. M. van der Steen, and J. S. van Wieringen, J. Phys. Chem. Solids 30, 799 (1969).